AIP ADVANCES **7**, 056411 (2017)

Enhancement of β-phase in PVDF films embedded with ferromagnetic Gd_5Si_4 nanoparticles for piezoelectric energy harvesting

Shane Harstad,[1,a,b] Noel D'Souza,[1,a] Navneet Soin,[2] Ahmed A. El-Gendy,[1,3]
Shalabh Gupta,[4] Vitalij K. Pecharsky,[4,5] Tahir Shah,[2] Elias Siores,[2]
and Ravi L. Hadimani[1]
[1]*Department of Mechanical and Nuclear Engineering, Virginia Commonwealth University, Richmond, Virginia 23284, USA*
[2]*Institute of Renewable Energy & Environment Technology, University of Bolton, Deane Road, Bolton BL3 5AB, United Kingdom*
[3]*Nanotechnology and Nanometrology Laboratory, National Institute for Standards (NIS), Giza 12211, Egypt*
[4]*Division of Materials Science and Engineering, Ames Laboratory, US Dept. of Energy, Ames, Iowa 50011-3020, USA*
[5]*Department of Materials Science and Engineering, Iowa State University, Ames, Iowa 50011-2030, USA*

(Presented 4 November 2016; received 23 September 2016; accepted 18 October 2016; published online 4 January 2017)

Self-polarized Gd_5Si_4-polyvinylidene fluoride (PVDF) nanocomposite films have been synthesized *via* a facile phase-inversion technique. For the 5 wt% Gd_5Si_4-PVDF films, the enhancement of the piezoelectric β-phase and crystallinity are confirmed using Fourier transform infrared (FTIR) spectroscopy (phase fraction, $F_{\beta,}$ of 81% as compared to 49% for pristine PVDF) and differential scanning calorimetry (crystallinity, ΔX_c, of 58% as compared to 46% for pristine PVDF), respectively. The Gd_5Si_4 magnetic nanoparticles, prepared using high-energy ball milling were characterized using Dynamic Light Scattering and Vibrating Sample Magnetometry (VSM) to reveal a particle size of ~470 nm with a high magnetization of 11 emu/g. The VSM analysis of free-standing Gd_5Si_4-PVDF films revealed that while the pristine PVDF membrane shows weak diamagnetic behavior, the Gd_5Si_4-PVDF films loaded at 2.5 wt% and 5 wt% Gd_5Si_4 show enhanced ferromagnetic behavior with paramagnetic contribution from Gd_5Si_3 phase. The interfacial interactions between Gd_5Si_4 and PVDF results in the preferential crystallization of the β-phase as confirmed *via* the shift in the CH_2 asymmetric and symmetric stretching vibrations in the FTIR. These results confirm the magnetic Gd_5Si_4 nanoparticles embedded in the PVDF membrane lead to an increased β-phase fraction, which paves the way for future efficient energy harvesting applications using a combination of magnetic and piezoelectric effects. *© 2017 Author(s). All article content, except where otherwise noted, is licensed under a Creative Commons Attribution (CC BY) license (http://creativecommons.org/licenses/by/4.0/).* [http://dx.doi.org/10.1063/1.4973596]

INTRODUCTION

Poly(vinylidene fluoride) (PVDF) is a well-known membrane material suitable for a wide range of applications such as in piezoelectric sensors, actuators, and energy harvesting systems due to its versatile piezo-, pyro-, and ferroelectric behaviors.[1–5] The PVDF films also exhibit excellent chemical resistance, good strength and biocompatibility, as well as low melting temperature; factors which make

---

[a] Noel D'Souza and Shane Harstad contributed equally to this work.

[b] Corresponding Author. Electronic mail: smharstad@vcu.edu.

them particularly appealing for low-power piezoelectric energy harvesting applications. PVDF can crystallize in up to four different phases: α, β, γ and δ. Among those, the α-phase with a configuration of trans gauche$^+$ trans gauche$^-$ *(tg^+tg^-)* is the most thermodynamically stabile.[3,4] The all-trans (*tttt*) piezoelectric β-phase, wherein the dipoles are aligned perpendicular to the chain axis, on the other hand, is ferroelectric and has the highest spontaneous polarization among all. Unlike common ceramic ferroelectric materials such as lead zirconium titanate (PZT) or lithium niobate, which are brittle and usually require high-temperature processing and fabrication techniques, the ferroelectric semi-crystalline polymers such as PVDF offer a wide variety of fabrication routes including melt-casting,[6] solvent-casting,[7] fiber extrusion,[2,8–10] electrospinning[11] and phase-inversion.[6,12] PVDF films with high fraction of the crystalline β-phase and, therefore, with high self-polarization and piezoelectric coefficient have been prepared using phase inversion at low temperatures.[4–6] Regardless of the actual processing route, achieving high concentration of the β-phase is usually the main processing goal, making the resulting material highly responsive to the applied stress/strain. Especially, with the miniaturization of devices and reduction in their energy requirements, harvesting of mechanical energy from the ambient and human body vibrations and its conversion to electrical energy using piezoelectric nanogenerators is becoming more and more attractive.[1,13]

The β-phase content can also be enhanced by additives, such as nanoparticles, that serve as nucleation and crystallization sites[14–16] In particular, previous studies on multiferroic nanocomposite films consisting of poly[(vinylidenefluoride-co-trifluoroethylene], P(VDF-TrFE), and $CoFe_2O_4$ nanoparticles have examined the ferroelectric, piezoelectric and magnetoelectric properties of materials as a function of composite thickness, concentration of the ferrite and the direction of applied magnetic field.[17,18] Andrew *et al.* showed that by adding the oxidic spinel Ni–Zn ferrite nanoparticles into PVDF, the β- and γ -phase, containing longer trans sequences were produced in the composite electrospun fibers.[19] In the work carried by Tsonos *et al.*, with an increasing Fe_3O_4 content, an almost linear increase in the β-phase content of the PVDF/Fe_3O_4 composites was observed for nanocomposite films prepared *via* high shear twin-screw compounding followed by compression moulding.[3,20] Here we report preparation of 2.5 and 5 wt% Gd_5Si_4-PVDF nanocomposite films using phase-inversion technique and characterization of their crystallinity, microstructural and magnetic properties. The addition of ferromagnetic Gd_5Si_4 nanoparticles[21] that have high magnetic moment offers a simple and facile route to facilitate the enhanced crystallization of the β-phase in the PVDF films, thus providing a pathway toward increasing the piezoelectric coefficient of the membranes.

EXPERIMENTAL DETAILS

Synthesis of Gd_5Si_4 nanoparticles

Synthesis process has been described in details elswhere.[21] Briefly, Gd_5Si_4 nanoparticles were synthesized using arc-melting of the stoichiometric mixture of Gd (purity 99.9 %) and Si (Cerac Inc., USA, >99.999%) under Ar atmosphere. The arc-melting process was repeated six times to ensure homogeneity. To obtain sub-micron Gd_5Si_4 particles, the as-cast material was first ground in an agate mortar and screened to obtain powders with particle size of 53 μm or smaller. Further reduction in the particle size was achieved by high energy ball-milling in a magneto ball-mill (Uni-Ball-Mill 5) operating under high impact mode for 8 hours without adding any liquid processing agent.

Synthesis of Gd_5Si_4 -PVDF films

The Gd_5Si_4-PVDF films were fabricated using the phase-inversion technique described elsewhere.[12] Briefly, a 20 wt% PVDF- *N, N*-dimethyl formamide (DMF) solution was prepared by heating at 70°C, with continuous and vigorous magnetic stirring for about 3 hr. Subsequently, the desired amount of Gd_5Si_4 nanoparticle powders were added to the solution to obtain a 2.5 and 5.0 wt% addition. The PVDF films were then deposited on Si substrates wherein a fixed volume (~1.5 mL) of the solution is spin-coated on to a Si wafer at 1000 rpm for 15 sec. This was followed by a quick immersion into a deionized water bath held at a quenching temperature of 20°C to eliminate the DMF via solvent anti-solvent interactions.[12] The as-prepared films were then washed thoroughly with water to remove any traces of solvent and then dried overnight in air at room-temperature before undertaking any further characterization. The complete removal of solvent was confirmed through FTIR analysis.

Characterization

The Gd_5Si_4 nanoparticles and Gd_5Si_4-PVDF films were analyzed for their morphology using scanning electron microscopy (SEM, Hitachi Model SU-70). The particle size measurements were carried out on a Nano ZS zetasizer (Malvern Instruments). The vibrational characteristics of the films were examined by FTIR spectroscopy (Thermo Scientific iS10 Nicolet). Vendor-provided OMINIC software was used to analyze the results, including the calculation of β-phase content. The spectra were recorded at a nominal resolution of ±1 cm^{-1} for a total of 64 scans. Differential scanning calorimetry (DSC) was used to investigate the crystallinity of the polymer films on a TA Instruments DSC Q2000. The samples, approximate weight 2 mg, were heated at 10 °C/min from 20 °C to 200 °C under 50 ml/min N_2 flow. Vibrating Sample Magnetometer (VSM, Quantum Design, 3T Versalab) and magnetic force microscope (Veeco Dimension Icon) were used to investigate the magnetic properties of the particles and the direction of the magnetization respectively. The open circuit voltage measurements of the samples were carried out using a home-made impact tester which transmitted approx. 2-3 N of force at controlled variable frequency (1-20 Hz).

RESULTS AND DISCUSSION

Microstructural characterization

The average particle size of the as-prepared Gd_5Si_4 powder measured by dynamic light scattering technique is 470±129 nm. The SEM micrograph shown in Fig. 1a illustrates the surface of a PVDF film loaded with 5 wt%-Gd_5Si_4 particles, and the morphology of the ball milled Gd_5Si_4 nanoparticles is shown in Fig. 1b. The distribution of nanoparticles within the polymer matrix is even and there is no apparent agglomeration. The DSC thermograms for the pristine PVDF pellets and the Gd_5Si_4-PVDF films are shown in Fig. 2a. Both the pristine PVDF pellets and films show a melting temperature, T_M, in the range of 172-174°C, with a slight lowering in the T_M of PVDF films. However, upon the addition of Gd_5Si_4 to the PVDF matrix, the T_M of the nanocomposite films is significantly reduced to a value of ∼166.8 °C, with shoulder-like structures appearing at both low and high temperature sides for all the film samples. In fact, the T_M of the Gd_5Si_4-PVDF films is approximately 6.8 °C lower as compared to that of pristine PVDF membranes. It is largely accepted in the literature that β-phase melting occurs in the range 165–172 °C; α-phase crystals in the range 172–175 °C with the γ-phase melting between 175 and 180 °C (all are marked in Fig. 2a).[12,16] The thermograms for the Gd_5Si_4-PVDF films are largely enclosed within the range of the 165-170 °C, corresponding to the dominant β-phase thus confirming that the lowering of the T_M can be attributed to the enhanced β-phase contents of the films. With the addition of Gd_5Si_4 nanoparticles to the PVDF matrix, an increase in the crystallinity values was observed, which was calculated according to Soin *et al.*,[12] the crystallinity increased from ∼38.6% for the starting PVDF pellets to approx. 46.8% (for pristine PVDF films) to nearly 58% for the 5 wt% Gd_5Si_4-PVDF films. It has been reported previously by various groups that the

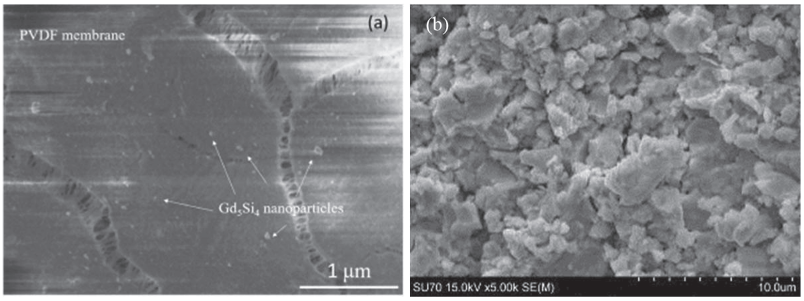

FIG. 1. (a) SEM image of the 5 wt% Gd5Si4-PVDF film prepared via phase inversion, (b) SEM image of the Gd_5Si_4 particles prepared via arc-melting and ball milling.

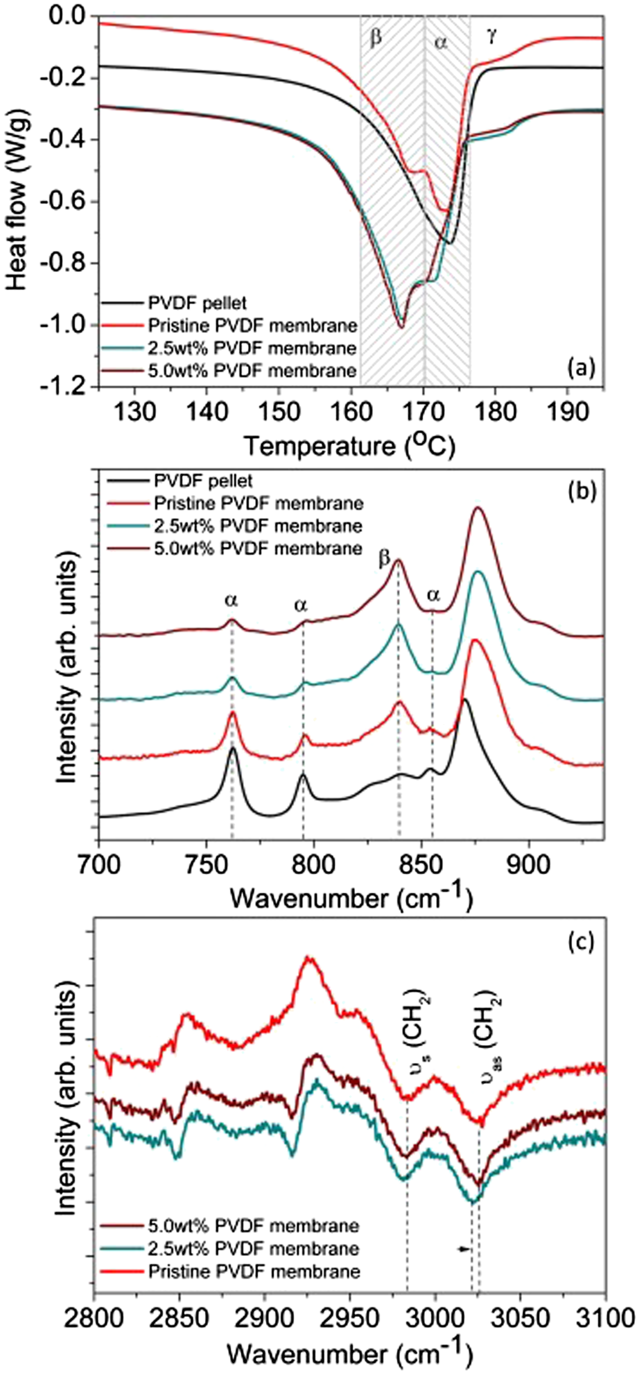

FIG. 2. (a) DSC thermograms with the melting zones of α, β and γ phases marked out, (b) FTIR spectroscopy measurements showing the enhancement of the β-phase with the addition of Gd_5Si_4 and (c) transmission spectra showing the shifts in the CH_2 symmetric and asymmetric mode of PVDF pellets, pristine PVDF, 2.5 wt% Gd_5Si_4-PVDF, and 5 wt% Gd_5Si_4-PVDF films.

addition of magnetic nanoparticles to the PVDF matrix can induce the nucleation of β-phase *via* static electronic interactions occurring between the magnetic particles with a negative zeta potential and the CH_2 groups with a surface positive charge density. Similar increase in the β-phase concentration has been observed by Martins *et al.*[22] in their study of $CoFe_2O_4/NiFe_2O_4$-PVDF composites where the addition of $NiFe_2O_4/CoFe_2O_4$ induced the all-trans configuration of the PVDF chains. In order to ascertain these interactions further FTIR measurements of the as-prepared films were carried out.

The measured FTIR spectra of the PVDF films are shown in Fig. 2(b) wherein the quantification of the β-phase in crystalline PVDF matrix relative to α-phase was carried out using the signature vibrational bands at 760 cm^{-1} (CF_2 bending and skeletal bending) and 840 cm^{-1} (CH_2 rocking and CF_2 asymmetric stretching vibration) using the procedure described in Ref. 12. Upon phase inversion, a significant increase in the β-phase is achieved for the PVDF membranes, wherein the β-phase concentration is enhanced to ∼49% from an initial value of ∼35% for the starting PVDF pellets. With the introduction of Gd_5Si_4 nanoparticles in the PVDF matrix, at the same processing conditions, the β-phase content is further enhanced to 71% and 80% for 2.5 and 5 wt% films, respectively. Furthermore, the interfacial electronic interactions occurring between the Gd_5Si_4 nanoparticles and the PVDF matrix were observed *via* the shifts in the CH_2 asymmetric and symmetric stretching vibrations modes as shown in Fig. 2(c). For the Gd_5Si_4-PVDF films, as compared to both pristine PVDF pellets and membranes, the asymmetric CH_2 (υ_{as}) vibrations showed a marked downshift from ∼3025 cm^{-1} to ∼3021 cm^{-1}, which has been attributed to the increase in the effective mass of the CH_2 dipoles resulting in the damping of the vibrational frequency.[23]

Magnetic measurements

The magnetic properties of the Gd_5Si_4 nanoparticles and Gd_5Si_4-PVDF nanocomposite film samples were determined using a VSM up to 3 T. The M-H hysteresis plots for the pristine, 2.5 and 5 wt% nanocomposite films at 300 K are shown in Fig. 3a. The pristine PVDF membrane shows diamagnetic behavior, while the films impregnated with Gd_5Si_4 nanoparticles exhibit behavior typical of ferromagnetism, which gets stronger with increasing nanoparticles concentration henceforth, we

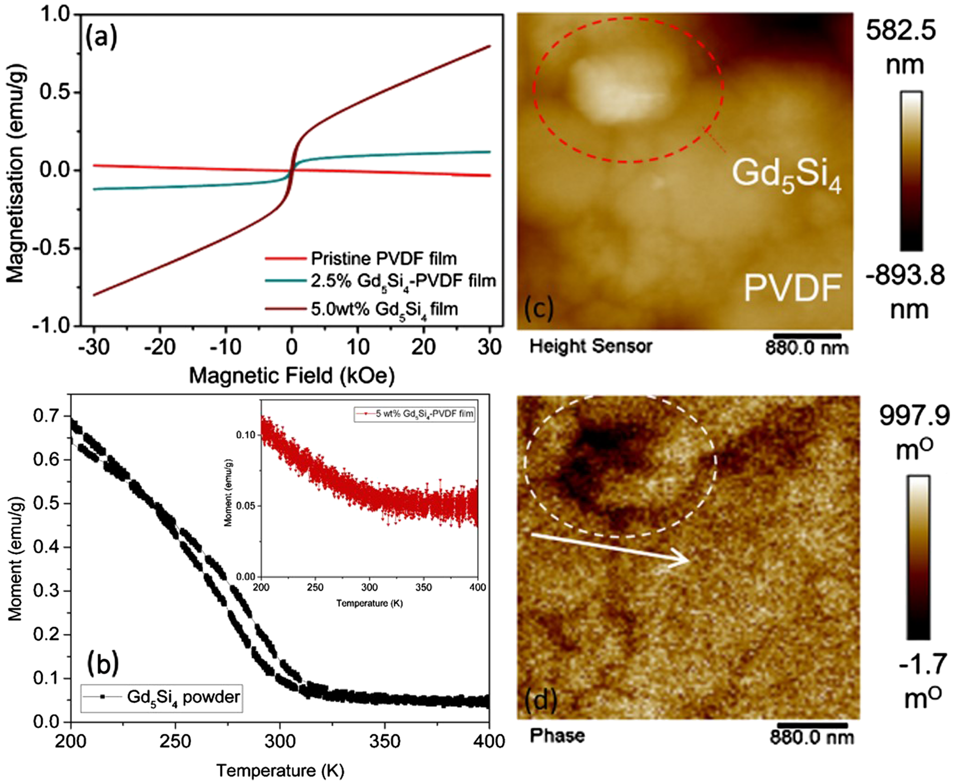

FIG. 3. (a) M-H hysteresis plots of the 5 wt% and 2.5 wt% Gd_5Si_4-PVDF samples compared with a pristine PVDF membrane. (b) M-T plot of the pristine Gd_5Si_4 nanoparticles, the inset shows the M-T plot of 5 wt% Gd_5Si_4-PVDF film. (c) AFM topography (upper) image of the 5 wt% Gd_5Si_4-PVDF membrane with the red circle highlighting a Gd_5Si_4 nanoparticle and (d) MFM phase image with the arrow showing the effective magnetization direction.

have focused mainly on the 5 wt% nanocomposite films. Magnetization as a function of temperature was measured at an applied field of 100 Oe for 5 wt% Gd_5Si_4 nanoparticles composite and for the Gd_5Si_4 nanoparticles alone as shown in Fig. 3b and in its inset respectively. It is observed that there is a reduction in the mass magnetization of the composite film due to the presence of non-magnetic PVDF however, the transition (slope of the curve) close to 300K is similar in both the samples indicating that there is no change in transition temperature. The low temperature part of the M vs. T graph shows a larger transition indicating the presence of a secondary Gd_5Si_3 phase in the particles but is not shown in the paper due to space limitation. Fig. 3c shows the atomic force microscopy (AFM) image of a Gd_5Si_4 nanoparticle in the PVDF membrane, along with the corresponding magnetic force microscopy (MFM) of the particle (Fig. 3d). The magnetization in the film is observed to be along the direction of the arrow shown in Fig. 3d. The difference in contrast inside the circled images displays the existence of different magnetic phases arising from Gd_5Si_3 and Gd_5Si_4 phases which in agreement with M vs. T measurements.

Voltage response

It is well established that the piezoelectric coefficient is directly proportional to the β-phase content and thus it can be argued that the 5wt% Gd_5Si_4-PVDF films should represent the highest

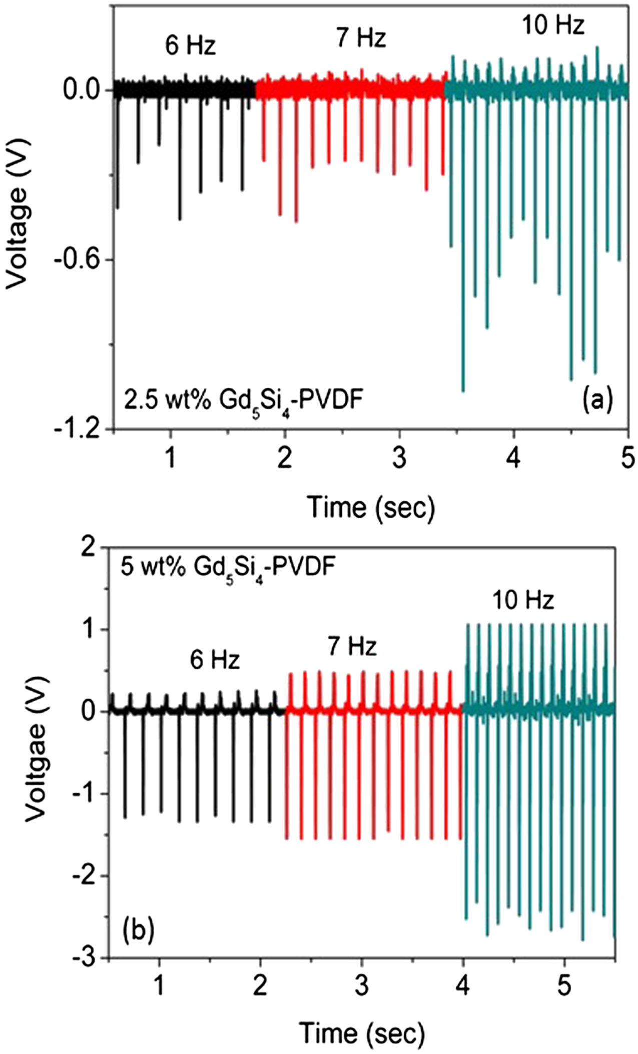

FIG. 4. Open circuit voltage measurements for the (a) 2.5 and (b) 5wt% Gd_5Si_4-PVDF film nanogenerators at a compression force of 2-3N from 6-10 Hz.

piezoelectric properties and voltage response to mechanical stimulations. To test this hypothesis, the nanocomposite film samples were assembled into nanogenerators using Indium Tin Oxide (ITO) deposited on PET polymer films as the top and bottom charge collectors. The samples were mechanically stimulated at a force of 2-3N at a frequency of 5-10 Hz (Fig. 4 a and b). As compared to the 2.5wt% nanocomposite film, the 5wt% film not only provides a significantly higher voltage output across the frequency range of 5-10 Hz but also a much more stable output which can be attributed to the enhanced content of the β-phase in the samples. Thus, the FTIR, DSC measurements in conjunction with the voltage response of the nanocomposite films are indicative of the positive effects of the addition of Gd_5Si_4 nanoparticles to the PVDF matrix in enhancing the β-phase and the crystallinity of the system.

CONCLUSIONS

Thin films of Gd_5Si_4–PVDF nanocomposite were successfully synthesized using phase-inversion method. The formed films were characterized in order to determine the increase in β-phase for potential energy harvesting applications. The enhancement of the piezoelectric β-phase and crystallinity are confirmed using FTIR and DSC. The interfacial interactions between Gd_5Si_4 and PVDF results in the preferential crystallization of the β-phase as confirmed via the shift in the CH_2 asymmetric and symmetric stretching vibrations in the FTIR. There is reduction in the net magnetization of composite film due to the presence of non-magnetic PVDF and the transition temperature of the composite film is similar which is around 300K. The composite film of PVDF-Gd_5Si_4 has resulted in an increased β-phase percentage which opens new root for their potential in future energy harvesting applications. Further work is needed to determine the nature of relationship quantitatively between the magnetization of nanoparticles on the volume fraction of β-phase in the Gd_5Si_4–PVDF nanocomposite films. For such a study, pure phase Gd_5Si_4 nanoparticles that have narrow particle size range are needed.

ACKNOWLEDGMENTS

This work is supported by the faculty start-up funds at the Department of Mechanical and Nuclear Engineering of the Virginia Commonwealth University. The work at Ames laboratory is supported by the Division of Materials Sciences and Engineering of Basic Energy Sciences Program of the Office of Science of the U.S. Department of Energy under Contract No. DE-AC02-07CH11358 with Iowa State University.

[1] S. Bauer, in *Electroresponsive Polym. Their Appl.* (Cambridge University Press, 2006), pp. 23–30.
[2] R. L. Hadimani, D. V. Bayramol, N. Soin, T. Shah, L. Qian, S. Shi, and E. Siores, Smart Mater. Struct. **22**, 75017 (2013).
[3] C. Tsonos, C. Pandis, N. Soin, D. Sakellari, E. Myrovali, S. Kripotou, A. Kanapitsas, and E. Siores, Express Polym Lett. **9**(12), 1104–1118.
[4] A. Bottino, G. Camera-Roda, G. Capannelli, and S. Munari, J. Memb. Sci. **57**, 1 (1991).
[5] D. J. Lin, K. Beltsios, T. H. Young, Y. S. Jeng, and L. P. Cheng, J. Memb. Sci. **274**, 64 (2006).
[6] K. M. Kim, N. G. Park, K. S. Ryu, and S. H. Chang, Electrochimica Acta **51**(26), 5636–5644 (2006).
[7] A. Salimi and A. A. Yousefi, Journal of Polymer Science Part B: Polymer Physics **42**(18), 3487–3495 (2004).
[8] N. Soin, T. H. Shah, S. C. Anand, J. Geng, W. Pornwannachai, P. Mandal, D. Reid, S. Sharma, R. L. Hadimani, D. V. Bayramol, and E. Siores, Energy & Environmental Science **7**(5), 1670–1679 (2014).
[9] D. Matsouka, S. Vassiliadis, K. Prekas, D. V. Bayramol, N. Soin, and E. Siores, Journal of Electronic Materials **45**(10), 5112–5126 (2016).
[10] D. Matsouka, S. Vassiliadis, D. V. Bayramol, N. Soin, and E. Siores, Journal of Intelligent Material Systems and Structures (2016).
[11] Z. Zhao, J. Li, X. Yuan, X. Li, Y. Zhang, and J. Sheng, Journal of Applied Polymer Science **97**(2), 466–474 (2005).
[12] N. Soin, D. Boyer, K. Prashanthi, S. Sharma, A. A. Narasimulu, J. Luo, T. H. Shah, E. Siores, and T. Thundat, Chemical Communications **51**(39), 8257–8260 (2015).
[13] Z. L. Wang and J. Song, Science **312**(5771), 242–246 (2006).
[14] D. Mandal, K. J. Kim, and J. S. Lee, Langmuir **28**, 10310 (2012).
[15] P. Martins, X. Moya, L. C. Phillips, S. Kar-Narayan, N. D. Mathur, and S. Lanceros-Mendez, Journal of Physics D: Applied Physics **44**(48), 482001 (2011).
[16] P. Martins, A. C. Lopes, and S. Lanceros-Mendez, Prog. Polym. Sci. **39**, 683 (2014).
[17] P. Martins, A. Lasheras, J. Gutierrez, J. M. Barandiaran, I. Orue, and S. Lanceros-Mendez, Journal of Physics D: Applied Physics **44**(49), 495303 (2011).

[18] P. Martins, C. M. Costa, and S. Lanceros-Mendez, Applied Physics A **103**(1), 233–237 (2011).
[19] J. S. Andrew and D. R. Clarke, Langmuir **24**(16), 8435–8438 (2008).
[20] C. Tsonos, N. Soin, G. Tomara, B. Yang, G. C. Psarras, A. Kanapitsas, and E. Siores, RSC Advances **6**(3), 1919–1924 (2016).
[21] R. L. Hadimani, S. Gupta, S. M. Harstad, V. K. Pecharsky, and D. C. Jiles, IEEE Trans. Magn. **51**, 5 (2015).
[22] P. Martins, C. Caparros, R. Gonçalves, P. M. Martins, M. Benelmekki, G. Botelho, and S. Lanceros-Mendez, The Journal of Physical Chemistry C **116**(29), 15790–15794 (2012).
[23] D. Mandal, K. Henkel, and D. Schreiber, Phys Chem Chem Phys **16**(22), 10403–10407 (2014).